Shear-induced mesostructure in nanoplatelet-polymer networks

S. Lin-Gibson, G. Schmidt,[a)] H. Kim,[b)] C. C. Han, and E. K. Hobbie[c)]
National Institute of Standards and Technology, Gaithersburg, Maryland 20899

The shear response of a model polymer–clay gel is measured using small-angle neutron and light scattering, optical microscopy, and rheometry. As the flow disrupts the transient network that forms between clay and polymer, coupling between composition and stress leads to the formation of a macroscopic domain pattern, while the clay platelets orient with their surface normal parallel to the direction of vorticity. We discuss similarities with shear-induced structural transitions observed in other complex fluids, and we offer a physical explanation for the orientation of the clay platelets. © *2003 American Institute of Physics.* [DOI: 10.1063/1.1609972]

I. INTRODUCTION

In response to the stresses induced by shear flow, a variety of complex fluids exhibit transitions to nonequilibrium phases of inherently lower symmetry. Examples include nematic-to-smectic-A transitions in liquid crystals,[1] sponge-to-lamellar transitions in surfactant systems,[2] and isotropic-to-lamellar transitions in block copolymers,[3] as well as shear-induced macrostructural transitions in semidilute polymer solutions,[4] wormlike micelles,[5,6] and bicontinuous microemulsions.[7] All of these systems exhibit flow-induced order out of an initially disordered or nanostructured equilibrium phase. In some, the shear induces microstructure in the form of smectic layers or lamellae,[1–3] while in others it induces phase separation in the form of macroscopic domains rich in one of the components.[4–7] Although theoretical models broadly addressing these nonequilibrium phases have been proposed,[8] a complete understanding of the underlying phenomena has yet to emerge.

As colloidal particles, clay nanoplatelets are particularly intriguing. Their sheetlike form makes them uniquely anisotropic, suggesting the possibility of novel liquid–crystalline phases associated with orientation of the platelets. When combined in solution with an adsorbing polymer, reversible short-range polymer–clay attraction can lead to a dynamic network, or physical gel, that is homogeneous on a macroscopic scale but heterogeneous on the nanoscale.[9] In this paper, we measure the shear response of these hybrid organic/inorganic gels using small-angle neutron scattering, light scattering, optical microscopy, and rheometry. As the shear distorts and ruptures the network, coupling between composition and stress leads to the formation of a macroscopic domain pattern, reminiscent of behavior associated with a number of other flow-induced structural transitions.[4–7] On smaller length scales, the clay platelets orient with their surface normal parallel to the direction of vorticity. We discuss similarities with the shear-induced structure observed in

other complex fluids,[2–7] and we suggest a physical scenario in which the clay orients in response to viscous and elastic stresses within macroscopic domains that represent intact remnant ''droplets'' of the equilibrium gel.

II. MATERIALS AND METHODS

Laponite LRD is synthetic hectorite clay composed of 30 nm diameter hydrophilic platelets of 1 nm thickness.[10,11] The polymer is poly(ethylene oxide) (PEO) of molecular mass 10^6 g/mol and mean radius of gyration[12] (R_g) 70 nm. The samples contain up to 3% (mass fraction) clay and up to 2% (mass fraction) polymer and were prepared by dissolving the LRD and PEO in distilled, deionized water. The pH is maintained at 10 via the addition of NaOH and the ionic strength is set at 10^{-3} mol/L NaCl. Solutions were gently mixed over the course of many weeks and were homogenous and optically transparent prior to use. Small-angle neutron scattering (SANS) measurements were performed on the 30 m SANS instrument at the NIST Center for Neutron Research using a Couette flow cell.[13,14] The geometry of shearing is in the x-y plane, with flow along the x axis, a constant velocity gradient along the y axis, and vorticity along the z axis. SANS probes the structure over the wave vector (q) interval 0.03 nm^{-1} $< q <$ 1.42 nm^{-1}, and two different geometries were used to procure measurements in both the x-z and y-z planes. Pure D_2O was used to enhance the combined scattering contrast of the polymer and clay, and H_2O/D_2O mixtures were used to contrast just the polymer.[9] Steady and dynamic rheology measurements were performed in cone-and-plate and parallel-plate geometries, respectively. A shear light-scattering/microscopy instrument provides real- and reciprocal-space measurements over length scales greater than 1 μm in the x-z plane.[15] Duplicate measurements on all instruments show excellent reproducibility.

The shear-induced orientation of platelets suggested by SANS is depicted in Fig. 1. In equilibrium, the adsorption of PEO segments onto the LRD surface[16] leads to the formation of a transient network or gel,[9] and the diffuse polymer chains thus serve as a way of ''bridging'' neighboring clay particles, which feel a short-range electrostatic repulsion.[10,11,16] The quiescent phase is thus disordered or *miscible* in the sense

[a)]Department of Chemistry, Louisiana State University, Baton Rouge, Louisiana 70803.
[b)]Department of Chemistry, Kyunghee University, Yongin, Kyungkido, Korea 449-701.
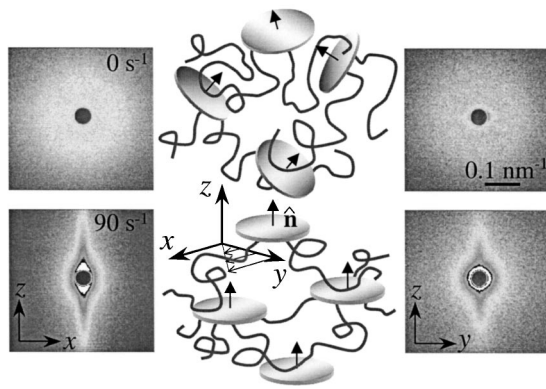[c)]Electronic mail: erik.hobbie@nist.gov

FIG. 1. Shear-induced orientation of platelets suggested by SANS, with the flow (x), gradient (y), and vorticity (z) directions, as indicated. In equilibrium ($\dot{\gamma}=0$, top), the platelets are randomly oriented and the SANS patterns in the x-z (top-left) and the y-z (top-right) planes are isotropic. Under these quiescent conditions, the adsorption of polymer segments onto the clay creates a physical gel. Under strong shear ($\dot{\gamma}=90$ s^{-1}, bottom) this network breaks, and the anisotropy of SANS patterns in the x-z (bottom-left) and y-z (bottom-right) planes suggests that the clay orients with its surface normal ($\hat{\mathbf{n}}$) parallel to the z axis. The sample depicted is 2% polymer and 3% clay in an aqueous solution at 25 °C.

that the samples are macroscopically homogeneous with ideal clay dispersion. The equilibrium SANS intensity, $S(q)$, exhibits a broad isotropic shoulder at $q_0 \approx 0.08$ nm^{-1}, corresponding to the equilibrium spacing between platelets[9] $d = 2\pi/q_0 \approx 80$ nm. At high shear rates ($\dot{\gamma}=\partial v_x/\partial y$) the anisotropy in the x-z and y-z planes becomes quite pronounced, reflecting the orientation of both clay and polymer. Measurements with the H_2O/D_2O ratio adjusted to highlight the response of just the polymer suggest that the clay is more susceptible to the orienting effect of the shear,[9] and the physical scenario is thus platelets that start to align with their surface–normal ($\hat{\mathbf{n}}$) parallel to the vorticity (z) axis (lower cartoon, Fig. 1) with increasing shear stress. Reference samples of pure 3% clay and pure 2% polymer show relatively little change under shear.

Optical measurements performed on analogous samples over the same range of $\dot{\gamma}$ suggest that the orientation described above is accompanied by a shear-induced macrostructure (Fig. 2). Information over length scales larger than 1 μm is obtained from both the light-scattering intensity, $S(\mathbf{q})$ (where 0.5 μm$^{-1} < q < 5$ μm^{-1}), and the computed correlation function $c(\mathbf{r}) = \langle \psi(\mathbf{r})\psi(0)\rangle$, where the field $\psi(\mathbf{r})$ (black regions, Fig. 2) denotes the local composition of macroscopic domains obtained from the optical micrographs.[17,18] Note that $S(\mathbf{q})$ and $c(\mathbf{r})$ are related by a Fourier transform. The absolute turbidity ($\lambda=632.8$ nm) is $\zeta = l^{-1} \ln(I_0/I)$, where l is the gap thickness, I_0 is the initial intensity, and I the transmitted intensity. ζ provides a measure of the average volume fraction of the segregated phase,[18] $\phi(\dot{\gamma})$. At intermediate shear rates (10–100 s^{-1}) the domains exhibit broad elongation along the vorticity axis and weak periodicity along the flow direction, as evidenced by well-defined correlation holes in $c(\mathbf{r})$ and winglike lobes in $S(\mathbf{q})$. The correlation lengths ξ_x and ξ_z characterizing the spatial coherence of the domain pattern are obtained by fitting projections to $c(x_i) \approx \exp(-2x_i/\xi_i)$ in the $x_i \rightarrow 0$ limit.[17] Projections of $S(\mathbf{q})$
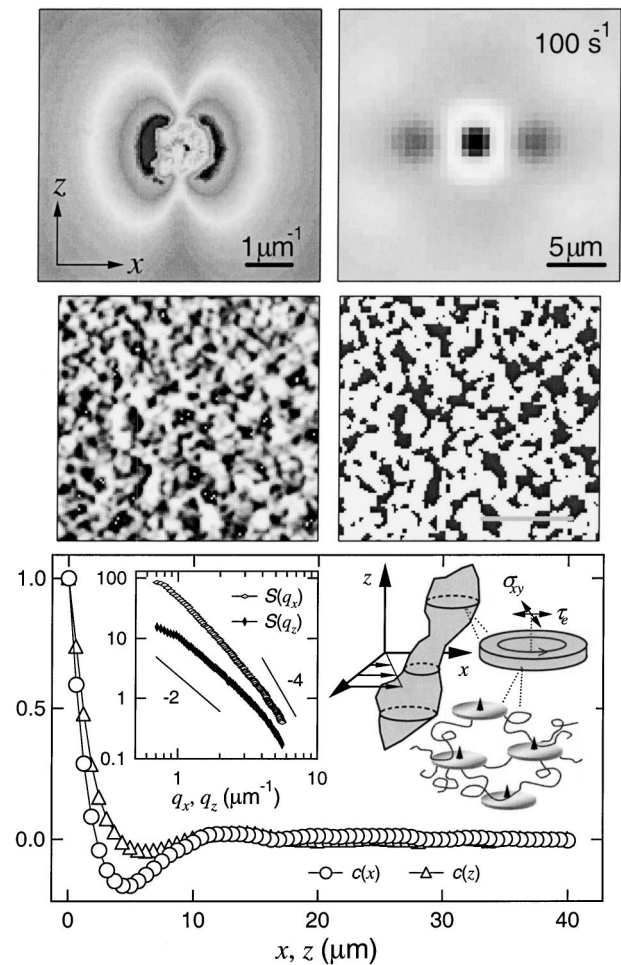

FIG. 2. Optical measurements of shear-induced macrostructure ($\dot{\gamma} = 100$ s^{-1}, analogous sample to Fig. 1) in the x-z plane. The upper-left image is the light-scattering pattern, $S(\mathbf{q})$. The middle-left image is the corresponding real-space micrograph, which yields a map (middle right, scale bar = 25 μm) of $\psi(\mathbf{r})$, the local composition of gel-like domains. The upper-right image is the two-point composition correlation function, $c(\mathbf{r})$, computed from $\psi(\mathbf{r})$. The lower figure shows projections of $c(\mathbf{r})$ along the flow (x) and vorticity (z) directions, and the inset shows analogous projections of $S(\mathbf{q})$. The cartoon depicts how biaxial stresses within one of the vorticity-aligned domains might orient the internal clay platelets in the manner suggested by SANS.

(inset, Fig. 2) exhibit a crossover to q_i^{-4} behavior at high q, indicative of sharp interfaces.[17] We attribute the appearance of well-defined macroscopic domains to a shear-induced breakup of the physical gel that forms in quiescence. Reference samples of pure polymer and pure clay show no change under shear.

III. RESULTS AND DISCUSSION

The mesoscale structural data are depicted in Fig. 3. The SANS anisotropy parameter is defined as $\Gamma_{ij} = [S(q_0\hat{\mathbf{x}}_i) - S(q_0\hat{\mathbf{x}}_j)]/[S(q_0\hat{\mathbf{x}}_i) + S(q_0\hat{\mathbf{x}}_j)]$ ($i,j = z,x$ or z,y) and the optical anisotropy parameter is defined as $(\Gamma_{zx})_\mu = (\xi_z - \xi_x)/(\xi_z + \xi_x)$. Also shown are $\zeta(\dot{\gamma})$ and $\phi(\dot{\gamma})$, where ϕ exhibits a maximum of around 0.20 in the vicinity of 100 s^{-1}. The microstructural anisotropy becomes quite developed in both planes as macroscopic phase separation proceeds. Initially, the structure (inset) exhibits modest elongation
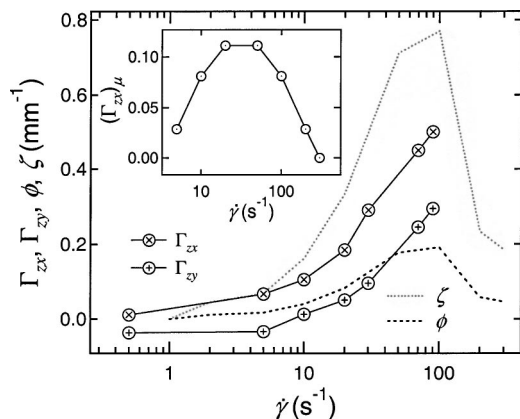
FIG. 3. The SANS anisotropy factors Γ_{zx} and Γ_{zy} as a function of $\dot{\gamma}$ for the sample depicted in Figs. 1 and 2 (2% polymer, 3% clay at 25 °C). The upper gray curve is the absolute turbidity, $\zeta(\dot{\gamma})$, and the lower black curve is the volume fraction of macrodomains, $\phi(\dot{\gamma})$, deduced from ζ. The inset shows the optical anisotropy factor $(\Gamma_{xz})_\mu$ obtained from the real-space optical data. Slightly negative values of Γ_{zy} at low $\dot{\gamma}$ are artifacts of curvature in the shear cell.

along the vorticity axis, but becomes isotropic with decreasing turbidity at high $\dot{\gamma}$. The mean correlation length, $1/2(\xi_x + \xi_z)$, stays roughly constant around 5 μm. A cartoon of the shear-induced mesostructure suggested by the morphological data, which spans five decades in length scale, is shown in Fig. 2. We suggest that, in general, the black gel-like domains experience a viscous shear stress, σ_{xy}, *and* an internal elastic stress, τ_e, where τ_e acts tangentially along closed internal streamlines in the *x-y* plane.[19] The latter stress is what leads to vorticity elongation in isolated droplets of viscoelastic fluid under shear in a less viscous and nonelastic suspending fluid.[19] We suggest that the "biaxial" nature of the total stress in the *x-y* plane might be what induces the observed orientation of the platelets (with $\hat{\mathbf{n}}$ parallel to the *z* axis), but more detailed computational work would be needed to validate such a simple and intuitive physical picture.

The rheology of these materials is revealing as well, with the response of the pure-clay solution itself being quite rich and complex. At concentrations as low as 1% LRD in water, the long-time "equilibrium" state is an orientational *glass* in which the platelets are not physically bonded to one another, but their rotational degree of freedom is frustrated by random packing.[10,20] For pure 3% clay, the small-amplitude dynamic response [Fig. 4(a)] exhibits solid-like behavior, with no terminal relaxation regime and a storage modulus $[G'(\omega)$, black] that exceeds the loss modulus $[G''(\omega)$, gray] over the measured range of angular frequency (ω). Applying steady shear causes the configuration of platelets to yield, and this yielding in turn leads to the constant shear-thinning behavior shown in Fig. 4(b), with $\eta \propto \dot{\gamma}^{-1}$ over more than six decades in $\dot{\gamma}$. By contrast, the pure 2% polymer behaves like a shear-thinning fluid, with a plateau at low $\dot{\gamma}$ and $G''(\omega) > G'(\omega)$ over the measured range of ω. For the composite samples, η dramatically increases with increasing clay concentration, until at 2% polymer and 3% clay (the same conditions as Figs. 1–3), an excess viscosity emerges at high $\dot{\gamma}$ that reflects the appearance of the macroscopic heterogeneities,
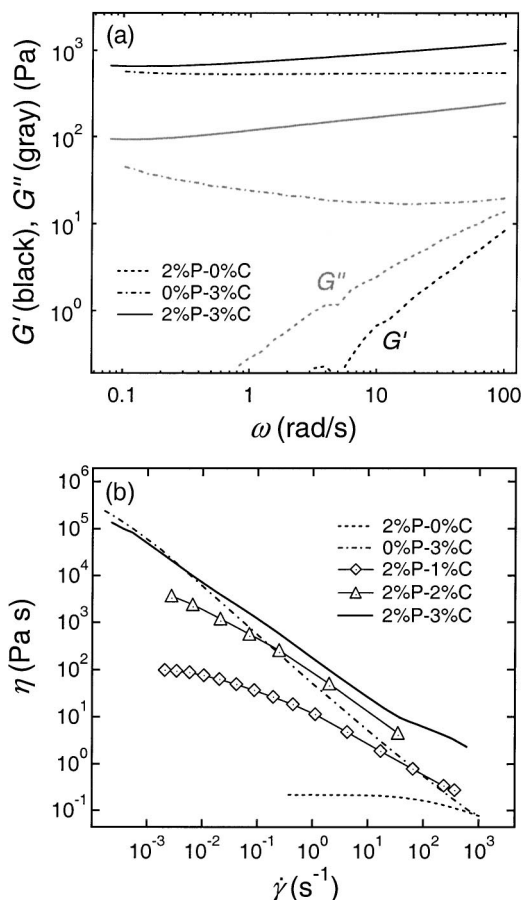

FIG. 4. (a) The loss $[G''(\omega)$, gray] and storage $[G'(\omega)$, black] moduli of a 2% polymer solution (lower dashed curve), a 3% clay solution (upper dashed curve), and the 2% polymer, 3% clay solution (solid curve). (b) Steady-shear viscosity as a function of $\dot{\gamma}$ for a 2% polymer solution, a 3% clay solution, and polymer–clay solutions (2% polymer) at various clay concentrations (1%, 2%, and 3% by mass) at 25 °C. Plots of σ_{xy} vs $\dot{\gamma}$ do not show a plateau with the transition.

$\psi(\mathbf{r})$. The physical network is evident in the dynamic viscoelastic response of the composite samples depicted in Fig. 4(a), which is enhanced with respect to that of the pure clay suspension.

IV. CONCLUSIONS

Although a more detailed quantitative model is desirable, the response can be qualitatively understood in terms of a critical shear rate, $\dot{\gamma}_c$. For $\dot{\gamma} < \dot{\gamma}_c$, the shear-induced reorientation of clay platelets is sufficiently slow such that the polymer chains have time to diffuse in a manner that accommodates yielding of the orientational glass, and η thus resembles that of the pure clay. For $\dot{\gamma} > \dot{\gamma}_c$, however, the platelets move faster than the polymer can diffuse, fragmenting the quiescent network into macroscopic domains. Note that the characteristic lifetime of the reversible polymer–clay attractive interaction is much faster than the time scales of relevance here.[9] An expression for $\dot{\gamma}_c$ can be derived by equating the time required for a platelet to translate the distance *d* in response to the flow with the time required for the polymer to diffuse the same distance. Assuming Stokes–Einstein diffusion, this yields $\dot{\gamma}_c \approx 2k_B T/6\pi \eta R_g d^2$. Taking η

as the viscosity of the pure (2%) polymer solution (which comprises the material between platelets) gives $\dot{\gamma}_c \approx 5 \text{ s}^{-1}$, in excellent accord with the data. Upon the cessation of shear, the domains quickly disappear and the samples become transparent, consistent with a time scale for "healing" on the order of $\dot{\gamma}_c^{-1} \approx 0.25 \text{ s}$. It takes much longer, however, for the low-$\dot{\gamma}$ rheological response to recover.

Although we note in passing that the orientation of the clay nanoplatelets is in stark contrast to the observed orientation of lamellae in the shear-induced sponge-to-lamellar transition, where the layers orient with their surface normal parallel to the gradient direction,[2] the transition observed here bears much more resemblance to the macroscopic phase segregation observed under shear in semidilute polymer solutions,[4] wormlike micelles[5,6] and polymeric microemulsions.[7] We suggest that the macroscopic domain pattern that accompanies such flow-induced heterogeneity might be more a reflection of the rheology of the two phases, and thus might not be an appropriate measure of universality within the admittedly broad scope of a shear-induced macrostructure. Rather, nanoscale heterogeneities with structural "connectivity" in a macroscopically homogeneous system would appear to be a common equilibrium or quiescent scenario, with phase separation then occurring when this structural coherence, mediated at the nanoscale by polymer entanglements, three-dimensional (3D) surfactant bilayers, or polymer "bridges" between particles, is interrupted by shear. Finally, we note that when the viscosity data in Fig. 4(b) are recast as shear stress versus shear rate, no stress plateau is observed with the transition, suggesting that although such a feature might be associated with shear banding,[5,8] it is not universal to biphasic effects in shear flow. We hope that the work described here will offer valuable physical insight into the broader phenomenon of shear-induced order in complex fluids and help guide the development of rigorous theoretical models of such behavior, particularly for systems exhibiting different types of flow-induced macroscopic phase separation.

ACKNOWLEDGMENTS

[1] C. R. Safinya, E. B. Sirota, and R. J. Plano, Phys. Rev. Lett. **66**, 1986 (1991).

[2] L. Pocar, W. A. Hamilton, P. D. Butler, and G. G. Warr, Phys. Rev. Lett. **89**, 168301 (2002); H. F. Mahjoub, C. Bourgaux, P. Sergot, and M. Kleman, *ibid.* **81**, 2076 (1998).

[3] K. Koppi, M. Tirrell, and F. S. Bates, Phys. Rev. Lett. **70**, 1449 (1993).

[4] E. Moses, T. Kume, and T. Hashimoto, Phys. Rev. Lett. **72**, 2037 (1994).

[5] J.-F. Berret, D. C. Roux, and P. Lindner, Eur. Phys. J. B **5**, 67 (1998).

[6] S. L. Keller, P. Boltenhagen, D. J. Pine, and J. A. Zasadzinski, Phys. Rev. Lett. **80**, 2725 (1998).

[7] K. Krishnan, K. Almdal, W. R. Burghardt, T. P. Lodge, and F. S. Bates, Phys. Rev. Lett. **87**, 098301 (2001).

[8] See, for example, P. D. Olmsted and C.-Y. D. Lu, Phys. Rev. E **56**, R55 (1997) and references therein.

[9] G. Schmidt *et al.*, Macromolecules **33**, 7219 (2000); *ibid.* **35**, 4725 (2002).

[10] M. Kroon, W. L. Vos, and G. H. Wegdam, Phys. Rev. E **57**, 1962 (1998).

[11] J. D. Ramsay, S. W. Swanton, and J. Bunce, J. Chem. Soc., Faraday Trans. **86**, 3919 (1990).

[12] K. Devanand and J. C. Selser, Macromolecules **24**, 5943 (1991).

[13] C. J. Glinka *et al.*, J. Appl. Crystallogr. **31**, 430 (1998).

[14] G. C. Straty, H. I. Hanley, and C. J. Glinka, J. Stat. Phys. **62**, 1015 (1991).

[15] S. Kim *et al.*, Rev. Sci. Instrum. **67**, 3940 (1996).

[16] J. Swenson, M. V. Smalley, H. L. M. Hatharasinghe, and G. Fragneto, Langmuir **17**, 3813 (2001).

[17] The field $\psi(\mathbf{r}) = 1$ or 0 if $\mathbf{r}$ falls inside or outside a domain, respectively. For a discussion of the link between this spatial pattern and the viscoelasticity of the dispersed phase, as well as details of the procedure used to extract the field $\psi(\mathbf{r})$ from the micrographs, see E. K. Hobbie *et al.*, J. Chem. Phys. **117**, 6350 (2002).

[18] See, for example, M. Kerker, *The Scattering of Light and other Electromagnetic Radiation* (Academic, London, 1969). For soft domains, we assume that ζ scales linearly with ϕ in the semidilute regime, where the constant of proportionality is obtained by assuming that the optimum threshold level at the highest turbidity gives an accurate measure of true area fraction in the micrographs, which is then used to estimate the volume fraction. The micrographs are thus thresholded in a manner that is consistent with the measured turbidity.

[19] In a reference frame that moves with a fixed volume element inside an isolated viscoelastic droplet, τ_e is constant and tensile, while the direction of principal shear stress appears to oscillate as the volume element rotates about the vorticity axis. For a discussion of τ_e and its relation to the droplet shape, see E. K. Hobbie and K. B. Migler, Phys. Rev. Lett. **82**, 5393 (1999); F. Migrhi and M. A. Huneault, J. Rheol. **45**, 783 (2001).

[20] F. Pignon, A. Magnin, J.-M. Piau, B. Cabane, P. Lindner, and O. Diat, Phys. Rev. E **56**, 3281 (1997).